BMC Genomics

RESEARCH

Open Access

Identifying insulin-responsive circRNAs in chicken pectoralis

Binghao Shao[1†], Ziyang Wang[1†], Pengna Luo[1], Pengfei Du[1], Xiangli Zhang[1], Huaiyong Zhang[1], Xuemeng Si[1], Sen Ma[1], Wen Chen[1*] and Yanqun Huang[1*]

Abstract

Background Circular RNAs (circRNAs) are stable, covalently closed non-coding RNAs formed by reverse splicing of precursor mRNA. They play critical roles in various biological processes, including insulin secretion and metabolism. However, their function in avian skeletal muscle's response to insulin remains poorly understood. This study aimed to comprehensively identify insulin-responsive circRNAs and explore their temporal and breed-specific regulation in poultry.

Results Using strand-specific RNA sequencing (ssRNA-Seq) on the pectoralis muscles of both Arbor Acres (AA) broilers and Silky fowls following insulin administration (5 IU/kg.BW, PBS as control). We identified 2,027 muscle circRNAs. Insulin-responsive circRNAs were detected in Silky fowls (29) and broilers (45) at 120 min, and in broilers (20) at 15 min post-injection. These circRNAs are enriched in processes such as exocrine pancreas development, response to exogenous stimuli, and regulation of intracellular signal transduction, likely mediated through a circRNA-miRNA network. Fewer insulin-responsive circRNAs were shared between time points in broilers (1) or between breeds (3) at 120 min. We further characterized a conserved insulin-responsive circRNA (circINSR), formed by exon 2 of the Insulin Receptor (*INSR*). The circINSR showed a similar spatiotemporal expression pattern to *INSR*, but exhibited distinct changes post-insulin administration. In broilers, *INSR* expression was dynamically modulated, while circINSR was downregulated only at 15 min ($P < 0.01$). Conversely, glucose did not change muscle circINSR but increased *INSR* at 10 min ($P < 0.01$). Energy restriction significantly downregulated circINSR ($P < 0.01$) without affecting *INSR* levels, and pyruvate had no effect on either circINSR or *INSR* levels.

Conclusion This study reveals the dynamic and breed-specific roles of circRNAs, particularly circINSR, in avian skeletal muscle's response to insulin. The distinct regulation of circINSR and *INSR* under various metabolic conditions suggests a complex regulatory mechanism. These findings provide novel insights into the molecular basis of insulin signaling in avian species and highlight the potential of circRNAs as biomarkers for metabolic regulation.

Keywords Insulin, Pectoralis muscle, CircRNA, *INSR*, Chicken

Background

Circular RNAs (circRNAs) are a unique class of endogenous non-coding RNA, formed through reverse splicing of precursor mRNAs, resulting in covalently closed circular transcripts [1, 2]. Unlike linear RNAs, circRNAs lacks a 5' cap and 3' poly A tail structure, which contribute to their remarkable stronger stability and resistance to RNase R [3]. To date, circRNAs have been reported to possess a various of functions, including regulating

†Binghao Shao and Ziyang Wang contributed equally to this work.

*Correspondence:
Wen Chen
cchenwen@aliyun.com
Yanqun Huang
hyanqun@aliyun.com
[1] College of Animal Science and Technology, Henan Agricultural University, Zhengzhou 450002, China

muscle cell development and adipocyte metabolism [4–6]. They exert their effects through multiple mechanisms, such as modulating mRNA transcription [7], binding to proteins [8], acting as microRNA (miRNA) sponges [9], and translating into proteins [10]. However, the functions of most circRNAs in animals remain largely unknown, making them an enigmatic class of RNA molecules.

Insulin is a hormone secreted by pancreatic β cells. It modulates a variety of biological processes in animals, including glucose transport, glycogen synthesis, amino acid transport, lipid metabolism and protein synthesis, ultimately promoting muscle growth [11, 12]. As the master regulator of glucose metabolism, insulin regulates blood glucose homeostasis through mediating glucose uptake in the insulin-sensitive tissues of animals, particularly in skeletal muscle [13]. Studies have shown that circRNAs could participate in regulating insulin secretion and synthesis [14–17], and some circRNAs have been linked to type II diabetes [18, 19]. Notably, an insulin-sensitive circRNA (circSfl) has been reported to possess the ability on regulating the lifespan of *Drosophila* [20].

In recent years, high-throughput RNA-sequencing technology (RNA-Seq) have revealed that chicken circRNAs are expressed in a stage-specific manner during development across multiple tissues, such as granulosa cells [21], pectoralis muscles [22, 23], abdominal preadipocyte [24], and the bursal of fabricius [25]. It has been reported that bird's circRNAs could be regulated by multiple exogenous stimuli, including NH_3 exposure in the thymus [26], infection with avian leukosis virus subgroup J in chick embryo fibroblasts [27], *Salmonella enterica* serovar Enteritidis infection in the cecum [28], Marek's disease virus infection in the spleen of chickens [29] and H5N1 avian influenza virus infection in chicken embryo fibroblast (DF1) cells [30]. However, to date, there have been no reports on the response feature of chicken circRNAs to exogenous insulin.

Birds exhibit unique glucose metabolism features compared to mammals, characterized by high fasting blood glucose concentrations (8–13 mmol/L) and strong insulin resistance [31, 32]. Arbor Acres (AA) broilers, a world-famous meat-type breed, grow rapidly and have heavy body weight and skeletal muscle content. In contrast, Silky fowls, a traditional Chinese medicinal breed characterized by black skin, exhibit slow growth and lower body weight along with reduced skeletal muscle content [33]. Our previous work demonstrated that AA broilers exhibited impaired regulation of blood glucose/insulin homeostasis, whereas Silky fowls show a stronger ability to regulate glucose homeostasis under exogenous insulin and glucose stimulation [33–35]. However, little is known about the transcriptional change in circRNAs induced by insulin in the skeletal muscle of birds, which is the primary site of insulin-dependent glucose disposal in animals.

With the development of high-throughput sequencing technology, insulin-sensitive circRNAs can now be screened under whole transcriptomics level using RNA Sequencing (RNA-Seq). Observing the changes in blood glucose levels following insulin application in broilers and Silky fowls led us to hypothesize that insulin may differentially regulate the expression of skeletal circRNAs between different administrated time points or breeds. Therefore, we systematically identified insulin-sensitive circRNAs through strand specific RNA Sequencing (ssRNA-Seq) with the pectoralis muscle of AA broilers at the early stage (15 min) and later stage (120 min) stages, as well as from Silky fowls at 120 min after insulin stimulation. Additionally, we also screened an insulin-sensitive circular RNA (circINSR), derived from exon 2 of the insulin receptor (*INSR*) gene and explored its expression characteristics. The identified insulin-responsive circRNAs will expand the candidate gene pool related to glucose homeostasis and muscle development in birds, laying the foundation for further investigation into their functions and the regulatory mechanisms of circRNAs.

Materials and methods

Ethics statement

The animal experiment scheme was approved by the Institutional Animal Care and Use Committee of Henan Agricultural University (HNND-2021–104, Zhengzhou, Henan, China). All animal experiments performed in this study comply fully with animal welfare regulations.

Experimental animals and sample collection

The fertilized eggs from Arbor Acres (AA) broilers and Silky fowls were artificially incubated according to general procedure. After hatching, the sex of the newly hatched chicks was determined through feather sexing for AA broilers and vent sexing for Silky fowls. Following sex determination, the chicks were reared in cages situated in an environmentally-controlled house. The house was maintained under a light regime of 23 h of light and 1 h of dark during the first week, shifting to 18 h of light and 6 h of dark thereafter. The ambient temperature was gradually reduced from an initial 32 °C down to 22 °C by Day 24 and maintained at this level for the remainder of the experiment. Throughout the study, the birds were provided with free and unlimited access to both food and water.

Except that the birds from feed restriction population were provided with the restricted diets (Table S1), the other AA broilers and Silky fowls were provided the same diets (Table S2) as described by Du et al. [33]. The nutrient composition of the diets met or exceeded the bird's

requirements as established in our previous experiment [33].

Insulin Tolerance Test (24 d): After a 12-h fasting period, 44 male broilers (approximately 800 ± 50 g) and 26 male Silky fowls (approximately 330 ± 30 g) were randomly selected and systematically divided into experimental and control groups for each breed. The experimental group birds were intraperitoneally injected with insulin (at a dosage of 5 IU/kg body weight, Insulin aspart Sanofi®, Novo Nordisk, China), while the control groups received comparable volumes of Phosphate Buffered Saline (PBS) solution [35]. Blood glucose levels were measured at 0, 15, 120, and 240 min post-injection (n = 10/group).

To avoid the interference with samples due to frequent blood glucose measurement after insulin administration, pectoralis samples were collected from another parallel broiler population at aforementioned time points (n = 6/time point/group), and from another parallel Silky fowl population at 120 min (n = 3/group). The collected samples were used for ssRNA-Seq and Real-Time Quantitative PCR (qRT-PCR) analysis.

Glucose Tolerance Test (18 d): Following a 12-h fast, male AA broilers (approximately 540 ± 50 g in body weight) were randomly selected and divided into the experimental group (n = 20) and control group (n = 20). Broilers in the experimental group were intraperitoneally injected with a 10% glucose solution, at a dosage of 2 g/kg body weight, while the control broilers received the same volume of normal saline. Blood glucose levels were mesured at 0, 10, 30, and 60 min (min) post-injection using a blood glucose meter (ACCU-CHEK Performa, Roche, Germany) [33, 36]. Pectoralis muscle samples were collected at 10- and 60-min post-injection (n = 6).

Pyruvate Tolerance Test (21 d): After a 12-h fast, male AA broilers (approximately 680 ± 50 g) were randomly selected and divided into experiment group (n = 20) and control group (n = 20). The experimental group was intraperitoneally administered with a sodium pyruvate solution at a dosage of 2 g/kg body weight, while the control group received an equivalent volume of normal saline solution [37]. Blood glucose concentrations were measured at 0, 10, 30, and 60 min post-injection and pectoralis muscles were collected at 0 min and 60 min post-injection (n = 6).

Feed restriction population (7-21d): the population for energy restriction and protein restriction were established as described in a previous study [38]. Briefly, sixty 7-day-old female AA broilers with similar body weight were randomly divided into three groups: 15% energy restriction group (n = 20), 15% protein restriction group (n = 20), and control group (n = 20). The diet for the control group was formulated based on chicken feeding standard recommendations for broilers (Peoples Republic of China, NY/T33-2004). The metabolic energy in the 15% energy restriction group was reduced to 85% of that of the control group. The crude protein content in the 15% protein restriction group was reduced to 85% of that of the control group, while other nutritional levels remained the same as those in the control group. Each group was provided with their respective diets. The composition and nutritional level of the experimental diets were shown in Supplementary Table S1. All birds were free to access feed and water throughout the experiment period. Pectoral muscles samples from each group (n = 5/group) were collected at 21d.

In addition, to examine the spatio-temporal expression profile of target genes, various tissues including the heart, liver, gizzard, glandular stomach, pectoralis muscle, leg muscle, brain, and pancreas, were collected from 21-day-old male broilers and male Silky fowls under a basal state (n = 5). Furthermore, pectoralis muscles samples were collected from broiler embryos at embryonic stage 10 (E10), and 19 (E19), as well as from male broilers at 21 d and 49 d post-hatching (under a basal state, n = 5). All samples were snap-frozen in liquid nitrogen and transferred to −80 °C refrigerator.

Library preparation and sequencing by ssRNA-seq

To investigate the dynamic and breed-specific responses of circRNAs to insulin stimulation, pectoralis muscle samples for ssRNA-Seq (n = 3/group) were collected from 24-day-old broilers at 15 min and 120 min after insulin (RI15, RI120) or PBS (RP15, RP120, control) injection, and from 24-day-old Silky fowls at 120 min after insulin (WI120) or PBS (WP120, control) injection (Fig. 1A). Total RNA was extracted from target samples using Trizol reagent (Invitrogen, CA, United States). The integrity of RNA was evaluated using a Bioanalyzer 2100 instrument with the RNA Nano 6000 Assay Kit (Agilent Technologies, CA, United States). RNA purity was checked using the NanoPhotometer® spectrophotometer (IMPLEN, CA, USA). RNA concentration was measured using Qubit® RNA Assay Kit on a Qubit® 2.0 Fluorometer (Life Technologies, CA, USA). A total of 5 μg RNA from each sample was used for screening circRNAs by ssRNA-Seq in each sample [22].

The ssRNA-Seq libraries were constructed using the NEBNext® Ultra™ Directional RNA Library Prep Kit for Illumina® (NEB, USA) following the manufacturer's recommendations. Ribosomal RNA was removed using the Epicentre Ribo-zero™ rRNA Removal Kit (Epicentre, USA). The first strand of cDNA was synthesized using random hexamer primers and M-MuLV Reverse Transcriptase (RNaseH-). DNA polymerase I

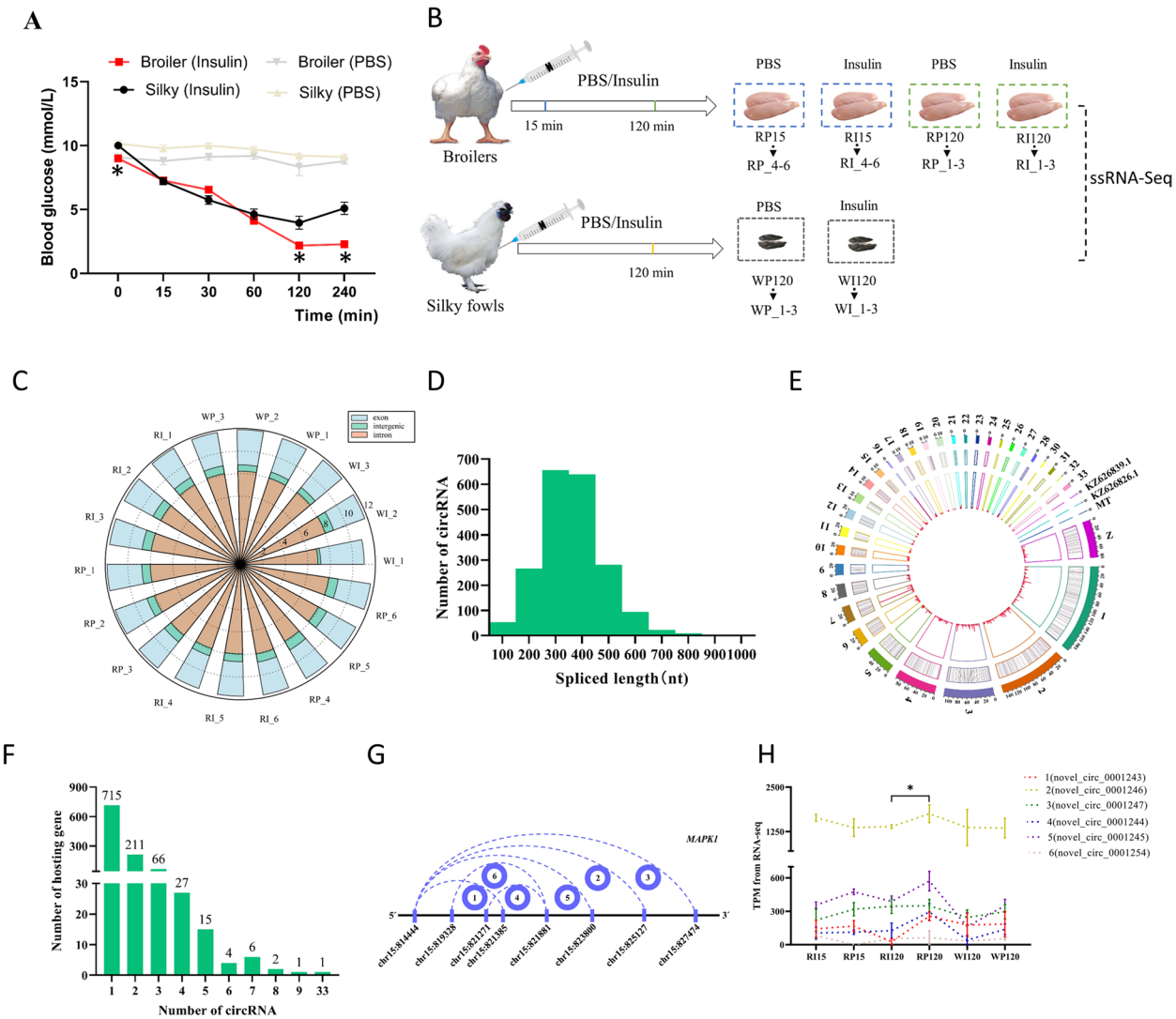

Fig. 1 Characterization and identification of circRNAs. **A** Dynamic changes in blood glucose levels in 24-day-old Silky fowls and AA broilers after insulin administration. *, $P < 0.05$ between two insulin- treated birds at a specific time- point. Birds were intraperitoneally injected with insulin at a dose of 5 IU/kg body weight, PBS- injected birds served as control. **B** Schematic representation of pectoralis sample collection for ssRNA-Seq. The samples were collected from the parallel insulin administration broilers and Silky fowls at the indicated time points, the naming of groups and individual samples was presented. **C** The source of circRNAs in each sample. **D** Spliced length (nt) distribution of circRNAs. **E** Distribution of circRNAs on each chromosome. The outer ring shows the chromosome map of chicken genome, while the inner rings represent the distribution of circRNAs on each chromosome. **F** Distribution of circRNAs in source genes. The X-axis represents the number of circRNAs that one mRNA gene can form. **G** Genomic diagrams of Six circRNAs formed by MAPK1. The number in circles denotes the corresponding circRNA presented in Fig. 1H. **H** Expression patterns of six circRNAs formed by MAPK1 among groups. For easy identification, the expression values of the same circRNA across groups are connected by the same color dashed line. "TPM" on the y—axis represents "transcript per million". *, $P < 0.05$

and RNase H were used to synthesize the second strand of cDNA. In the reaction buffer, dTTP was replaced by dUTP in the dNTPs mixture. The resulting product was purified by AMPure XP system, and the library quality was evaluated by Agilent Bioanalyzer 2100 system. Finally, the library was sequenced on an Illumina HiSeq 6000 (Novogene, Beijing, China).

Identification of differentially expressed circRNAs (DECs)

Fastp v 0.19.3 was used to filter the original data. Clean data (clean reads) were achieved by filtering reads containing adapter and low-quality reads from raw data, and then they were mapped to chicken genome (http://ftp.ensembl.org/pub/release-105/fasta/gallus_gallus/dna/, GRCG6a) with Bowtie2 v2.2.8 [39]. Transcript assembly was performed with Cufflinks software (http://cole-trapn

ell-lab.github.io/cufflinks/). Find_circ and CIRI2 software were used to identify circRNAs [40, 41]. The overlapping circRNAs identified by two tools were considered as candidates [42]. TPM method (transcripts per million) was used to normalize the expression of circRNAs [43]. DECs were identified by DESeq R package (version 1.10.1) [44] for the following comparisons: RI15_vs_RP15, RI120_vs_RP120, RI120_vs_RI15, RP120_vs_RP15, WI120_vs_WP120. Finally, circRNAs with $P < 0.05$ were considered statistically significant DECs.

Enrichment analysis on source genes of DECs

Emerging reports have shown that the functions of circRNAs may be associated with the parental linear transcripts [45]. To annotate the potential functions of circRNAs, all source genes of DECs were aligned against the Gene Ontology (GO) databases and the Kyoto Encyclopedia of Genes and Genomes (KEGG) database. GO enrichment analysis was performed using the GOseq R package [46], and KEGG pathway enrichment analysis was performed using Kobas software [47]. A P-value < 0.05 was set as the significance threshold. The top 20 KEGG pathways and top 10 GO terms (biological process) are presented. All the GO and KEGG enrichment results are shown in Table S7 and Table S8.

The potential function prediction of circRNAs

CircRNAs can function as efficient microRNA sponges [48]. Therefore, miRanda was used to predict the miRNA binding site of the spliced circRNAs, and the circRNA-miRNA interaction network was constructed using the top 10 DECs (based on |log2FoldChange| values) from all comparison combinations with Cytoscape 3.6.0. Internal ribosome entry site (IRES) can directly recruit ribosomes to initiate translation in a cap-independent manner [49]. IRES finder software was used to detect whether the circRNAs contain IRES elements and to predict their potential for initiating translation without relying on the 5' cap structure. A score of 0.5 was set as the threshold for evaluating translation potential with scores closer to 1 indicating higher reliability. The circRNA-miRNA interaction network was constructed using the top 10 DECs (based on |log2FoldChange| values) from all comparison combinations.

Experimental verification of circRNAs

Seven DECs were randomly selected from RNA-Seq data. Their cyclic properties and expression levels were further validated using three approaches. First, divergent primers and convergent primers (Table S3) were designed to distinguish the expression of circRNAs and their source genes, using cDNA and genomic DNA (gDNA) as templates, respectively. The PCR products were detected by agarose gel electrophoresis. Second, the back-splice junction was validated through sanger sequencing (Sangon, Shanghai, China). Third, the stability of circRNAs was further confirmed by qRT-PCR using RNase R-treated total RNA (Geneseed, Guangzhou, China) in RP120 group. Additionally, the expression of these circRNAs in all groups were further validated by qRT-PCR. Here the validated circRNAs were renamed according to their source genes (Table S3). Divergent primers were designed based on the 100–200 bp sequence overlapping with the junction site, while convergent primers were designed based on one exon of the source gene.

qRT-PCR

Total RNA was extracted from target tissues using Trizol reagent (TRANS, Beijing, China) following the manufacturer's instructions. The RNA quality was assessed using the NanoPhotometer® spectrophotometer (IMPLEN, California, USA) and agarose gel electrophoresis. A total of 1 μg RNA was reverse transcribed to obtain cDNA using HiScript ® III 1st Strand cDNA Synthesis Kit (Vazyme, Nanjing, China). The reverse transcription process contained two steps. The first step was to remove genomic DNA: total RNA 1 μg, 5×gDNA wiper Mix 2 μL, supplemented with ddH_2O to 10 μL and incubated at 42 °C for 2 min. The second step was to synthesize cDNA: step one product, 2 μL of 10×RT Mix, 2 μL of HiScript III Enzyme Mix, 1 μL of $Oligo(dT)_{20}VN$, 1 μL of Random hexamers, and 4 μL of ddH_2O. Then they were incubated at 37 °C for 15 min and 85 °C for 5 s.

The qRT-PCR was performed to determine the mRNA level of target genes on BioRad CFX96 (BioRad, USA) using ChamQ Universal SYBR qRT-PCR Master Mix (Vazyme, Nanjing, China). The primers (Table S3) were optimized to ensure high amplification efficiency. The *β-actin* was used as a housekeeping gene to normalize the expression of target genes. The qRT-PCR reaction system consisted of cDNA 50 ng, forward and reverse primers 0.2 μL, ChamQ Universal SYBR qPCR Master Mix 5 μL, supplemented with enzyme-free water to 10 μL. The qRT-PCR procedure consisted of the following steps: an initial denaturation at 95 °C for 5 min, followed by 38 cycles of denaturation at 95 °C for 30 s, annealing at 60 °C for 30 s, extension at 72 °C for 30 s, and a final extension at 72 °C for 1 min. The amplification without template cDNA was set as the negative control. Each sample was repeated at least three times. The relative expression level of target genes was normalized to the reference gene calculated based on the $2^{-\Delta\Delta Ct}$ method [50].

Statistical analysis

The qRT-PCR data were analyzed using SPSS statistical software version 26.0 (Inc, Chicago, IL, USA). Upon

verifying the normal distribution and variance homogeneity of the data, one-way ANOVA was employed, followed by Tukey post hoc tests, for the comparison of multiple data sets. Additionally, Student's t-tests were utilized for the comparison between two data sets. Data were expressed as mean ± standard error (SEM). A $P < 0.05$ was considered statistically significant. GraphPad Software (Version 8.0, La Jolla, CA, United States) was used to visualize the data.

Results

Blood glucose drop in a breed-specific manner under insulin administration

A sharp decline in blood glucose is observed over time in birds after insulin administration. However, two breeds presented distinct modulation pattern response to insulin with time. The basal blood glucose levels in broilers were lower compared to Silky fowls ($P < 0.05$). After insulin administration, the blood glucose levels in broilers rapidly decreased continuously up to 120 min, and remained low up to 240 min. However, the blood glucose levels in silkie chickens began to gradually rise after 120 min. The blood glucose levels in broilers were significantly lower than those in Silky fowls at 120 min ($P < 0.05$) and 240 min ($P < 0.05$) post-insulin administration (Fig. 1A). On the other hand, birds in the PBS control group maintained relatively constant blood glucose levels throughout the observation period (Fig. 1A).

Identification of circRNAs by ssRNA-seq and experimental validation

Based on the observed changes in blood glucose levels post-insulin stimulation in AA broilers and Silky fowls, circRNA transcriptome sequencing was performed on pectoral muscle samples from broilers at 15 and 120 min post-stimulation to examine the time-dependent effects of insulin action. Additionally, circRNA transcriptome sequencing was conducted on pectoral muscle samples collected from Silky fowls at 120 min post-stimulation (with PBS as the control) to investigate the breed-specific difference in insulin response mechanisms by comparing the sequencing data with that of broilers at the same time point (Fig. 1B).

A total of 2,027 circRNAs were identified by ssRNA-Seq from 18 pectoralis cDNA libraries (Fig. 1 and S1, Table S4). It showed that most of the circRNAs originated from genes, therein, 81.5% of circRNAs formed by exons and 7.6% was from introns, only 10.9% of circRNAs were in intergenic regions (Fig. 1C and S1A). Most circRNAs consist of two or three exons (Fig. S1B). After splicing, the longest circRNA was 1000 nucleotides (nt), the shortest was only 100 nt, while the majority were between 200–500 nt (Fig. 1D). The circRNAs are widely distributed on all chromosomes, especially on chromosome 1 (Fig. 1E and S1C), which may be related with the length of the chromosome (Fig. S1D). In addition, a circRNA (novel_circ_0010996) was detected from the 16S ribosomal RNA region of chicken mitochondria (Table S4). Of the 2,027 identified circRNAs, 68.23% of genes only produce one circular RNA, while the remaining genes produce two or more circular transcripts. In fact, there are cases where a single gene can produce up to 33 different circular transcripts (Fig. 1F, Table S4).

We randomly selected 7 circRNAs from ssRNA-Seq data to confirm their cyclization characteristics through agarose gel electrophoresis, Sanger sequencing, and qRT-PCR. As expected, the divergent primers for amplifying circular RNA produced bands in the system containing cDNA template but not gDNA template. Conversely, the amplification with convergent primers produced bands in both the system containing cDNA template and gDNA template (Fig. 2A). Sanger sequencing further confirmed the back-splicing junctions of these circRNAs (Fig. 2B). The qRT-PCR revealed there was no significant difference in the expression of circRNAs between the RNase R-treated samples and the control samples (Fig. 2C). However, the expression levels of the corresponding linear source genes and *β-actin* decreased significantly after treatment with RNase R, indicating that circRNAs are relatively stable and resistant to RNase R degradation (Fig. 2D). In addition, the expression of these circRNAs detected by qRT-PCR, was consistent with the ssRNA-Seq results overall, which confirmed the reliability of the RNA-Seq data (Fig. 3).

Characteristics of identified circRNAs by ssRNA-seq

We analyzed the global expression characteristics of identified circRNAs using ssRNA-Seq. Density analysis showed that the expression abundance of most circRNAs concentrated in the ranges of TPM < 0.1 and TPM > 60 (Fig. S2A). The circRNAs with TPM > 60 accounts for approximately 70% (Fig. S2B, Table S4). The top three circRNAs (based on TPM value) were novel_circ_0009745, novel_circ_0009733, and novel_circ_0009716. These circRNAs varied in sequence length, but, in fact, originated from the same intergenic region of chromosome 7 (Table S4). Their average TPM values were 809,200, 58,957, and 25,800, respectively. It was found that the abundance of each circular transcript varied depending on its formation mode. For example, six circRNAs originating from mitogen-activated protein kinase 1 (*MAPK1*) gene exhibited distinct abundance and differential expression among groups (Fig. 1G and 1H, Table S5). Among these, novel_circ_0001246 had high TPM values across groups and was significantly downregulated by insulin

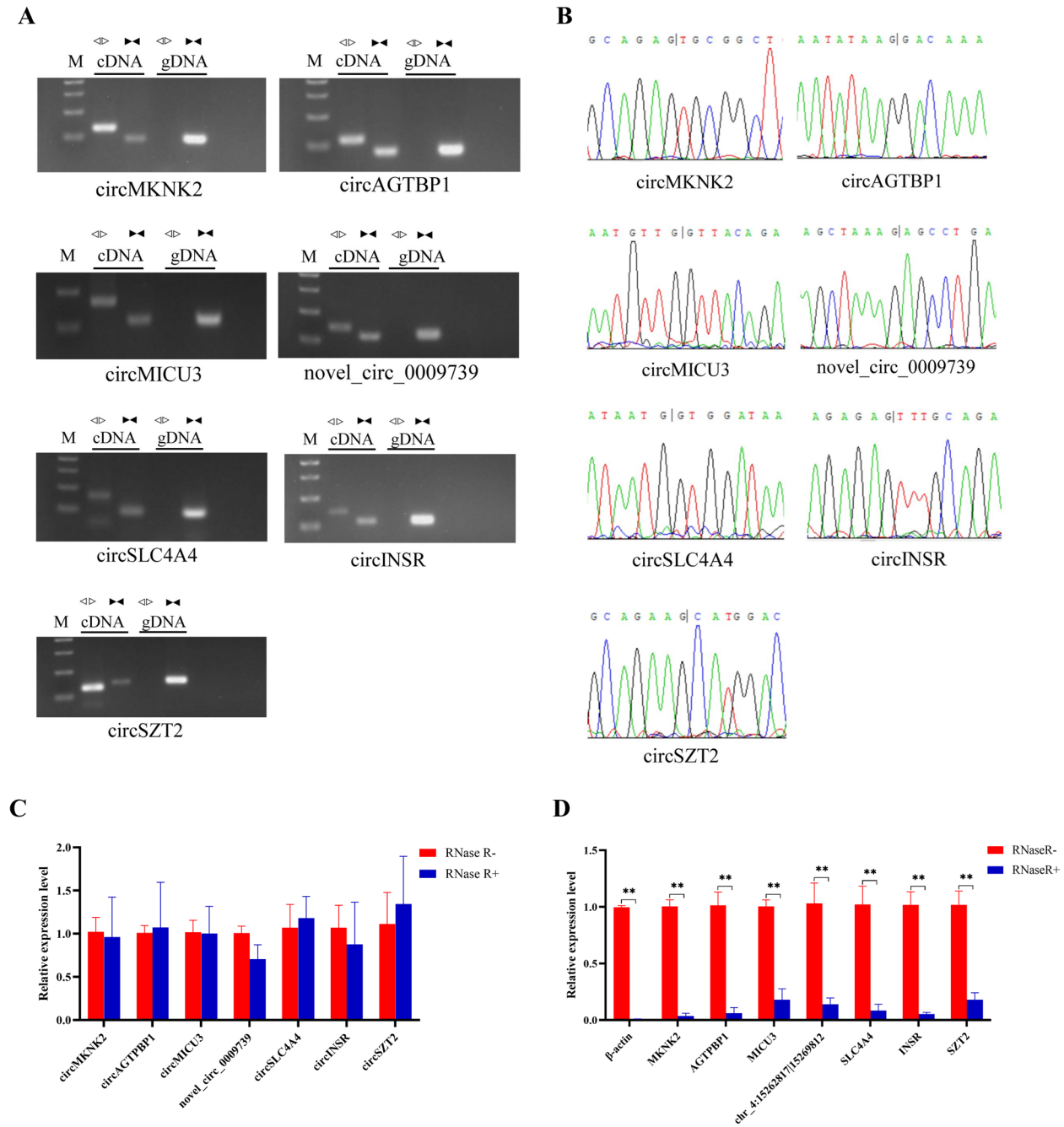

Fig. 2 The experimental validation of circRNAs. **A** CircRNAs and their source genes were amplified using cDNA and genomic DNA (gDNA) as templates with Convergent and Divergent primers, respectively. "◁▷" represents Convergent primers for amplifying circRNAs; "►◄" represents Divergent primers for amplifying the source gene, and "M" represents DNA Maker. **B** Sanger sequencing confirmed the junction sites of circRNAs. the back-splicing junction positions are marked with short lines. Comparison of the expression levels of circRNAs **C** and their source genes **D** before and after RNase R treatment. **, $P < 0.01$

administration at 120 min ($P < 0.05$, Fig. 1H). However, the relative expression of novel_circ_0001254 was very low, and its expression was even undetectable in RP15 group (Fig. 1H).

DECs identified by insulin stimulation from chicken pectoralis

In the broiler population, 20 circRNAs (9 upregulated and 11 downregulated) were significantly regulated at

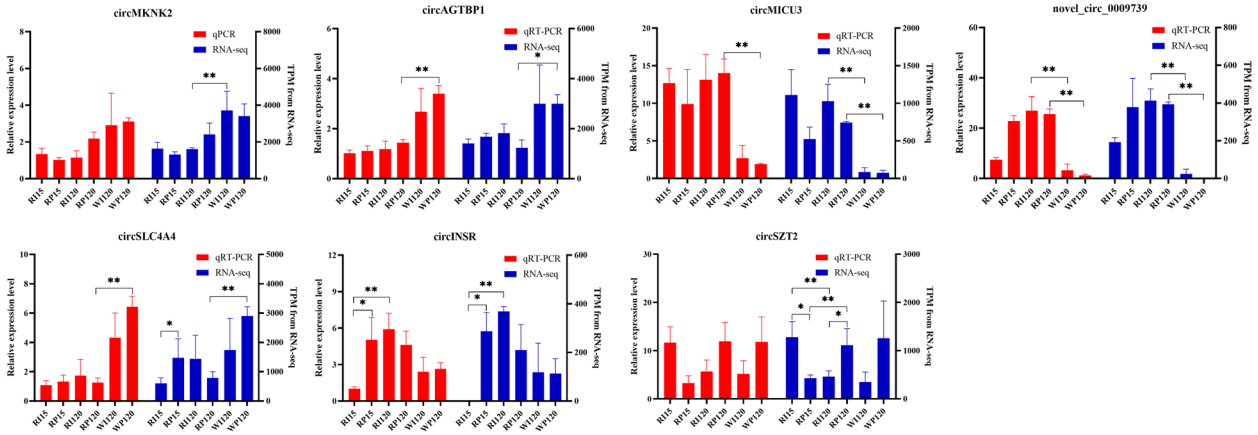

Fig. 3 Validation of differentially expressed circRNAs (DECs) by qRT-PCR. The red column represents the expression data detected by qRT-PCR ($n = 3$), and the blue column represents the expression level from ssRNA-seq data ($n = 3$). *, $P < 0.05$; **, $P < 0.01$

15 min after insulin stimulation (RI15_vs_RP15). Notably, the level of novel_circ_0004546 (named circINSR based on its original gene *INSR*) significantly decreased in response to exogenous insulin (Fig. 4A, Table S4). With the passage of time, a larger number of circRNAs were significantly affected by exogenous insulin. At 120 min (RI120_vs_RP120), 17 circRNAs were up-regulated and 28 were down-regulated in response to exogenous insulin (Fig. 4B, Table S4). It is worth noting that only one circRNA (novel_circ_0010459, circSZT2) was significantly altered by exogenous insulin at both 15 min (RI15_vs_RP15, up-regulated) and 120 min (RI120_vs_RP120, down-regulated). However, its expression changed in opposite directions at the two time points (Fig. 4F, Table S4).

We further analyzed the dynamic change of circRNAs over time after insulin and PBS injection in broilers individually. The genes, that are specifically regulated by insulin over time, are referred to as time-dependent insulin-responsive genes here. It was observed that 38 circRNAs (18 upregulated and 20 downregulated) changed over time with insulin action (RI120_vs_RI15, Fig. 4C). Therein, the novel_circ_0004546 (circINSR) was dramatically upregulated with time (top one, Fig. 4C). Meanwhile, some circRNAs (31 upregulated, 21 downregulated) also changed with time in birds injected with PBS solution (RP120_vs_RP15, Fig. 4D). Nonetheless, Venn analysis revealed that only two time-dependent DECs (circSZT2 and novel_circ_0001237) were shared between the insulin-treated and PBS-injected birds (Fig. 4F). Therein, circSZT2 was the only differentially expressed gene shared across four comparisons in broilers (Fig. 4F). However, the expression of circSZT2, which was up-regulated over time in PBS control birds (RP120_vs_RP15), was reversed by insulin stimulation (RI120_vs_RI15) (Figs. 3F and 4F, Table S4).

To investigate the effect of breed on birds' response to insulin, we further identified the insulin-sensitive DECs from Silky fowls (at 120 min after insulin administration). Compared to the PBS control, 6 DECs were upregulated and 23 DECs were down-regulated at 120 min after insulin injection in Silky fowls (WI120_vs_WP120, Fig. 4E and Table S4). Venn analysis revealed that most insulin-sensitive DECs at 120 min were regulated in a breed-specific manner, with 42 insulin-sensitive DECs were specific to broilers, and 26 insulin-sensitive DECs specific to Silky fowls) (Fig. 4G). Among these, three common DECs (novel_circ_0004076, novel_circ_0010996, and novel_circ_0001431) were down-regulated by exogenous insulin in both breeds (Fig. 4G and H, Table S4). Specifically, the novel_circ_0004076 originated from cell division control protein 42 homolog (*CDC42*) gene, novel_circ_0010996 was derived from mitochondrial 16S ribosomal RNA, and novel_circ_0001431 was from Zinc Finger Protein 425 (ZNF425).

Functional enrichment analysis of genes derived from DECs

We conducted GO/KEGG enrichment analysis based on the source genes of the identified DECs. The top 10 GO terms related to biological processes (Fig. 5, Table S7) and the top 20 KEGG pathways (Fig. 6, Table S8) were presented for each comparison. In broilers, at 15 min after exogenous insulin stimulation (RI15_vs_RP15), GO terms such as exocrine pancreas development and response to cell cycle checkpoint signaling were enriched (Fig. 5A, Table S7). At 120 min after insulin stimulation, abundant GO items were found to be enriched in processes related to the regulation of the response to exogenous stimulation, including glucose/amino acid starvation and nutrient levels in RI120_vs_RP120 and RI120_vs_RI15 comparisons (Fig. 5A, Table S7).

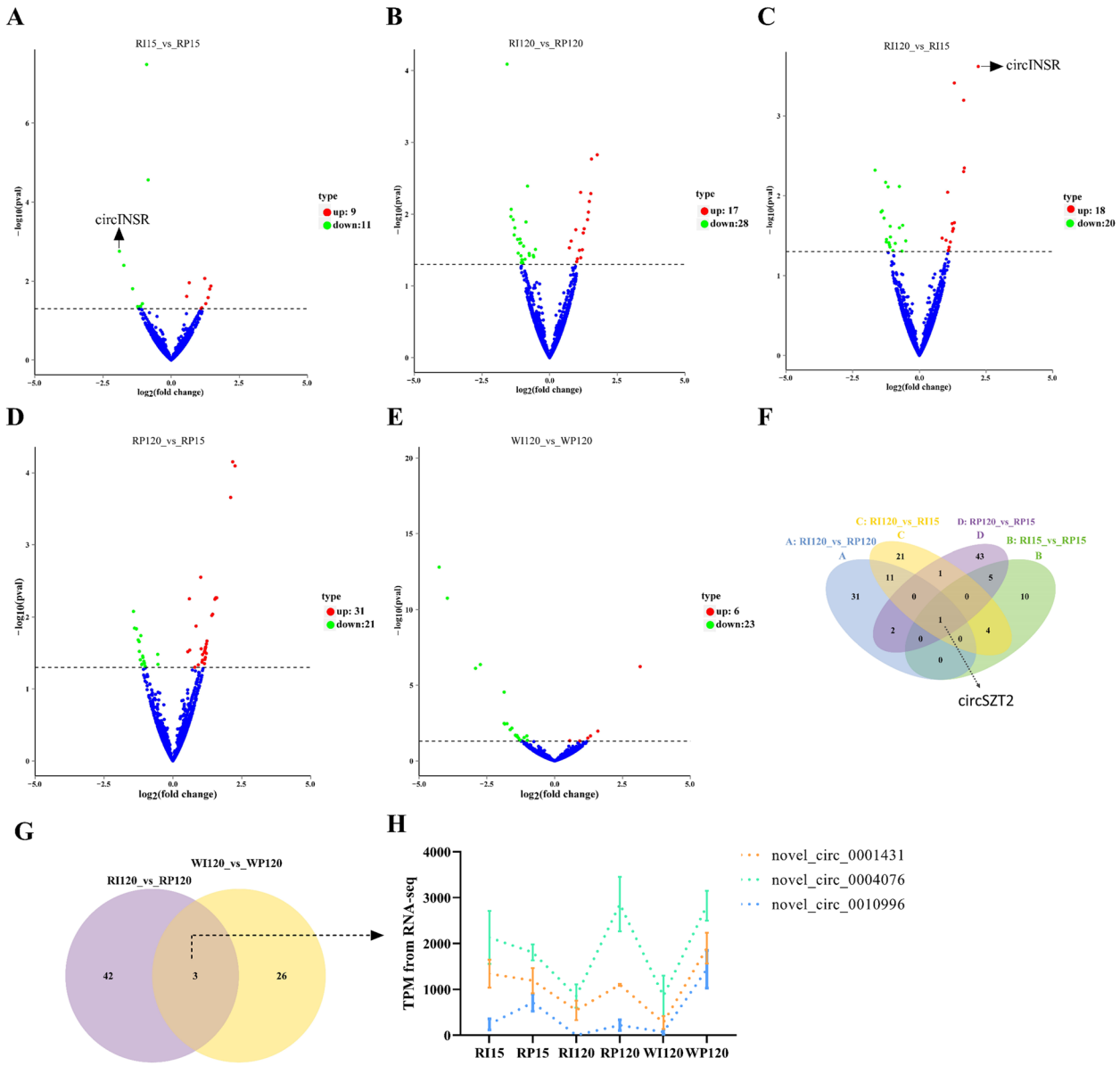

Fig. 4 Identification of DECs in chicken pectoralis after insulin stimulation. **A-E** The volcano map for the following comparisions (**A**) RI15_vs_RP15, **B** RI120_vs_RP120, **C** RI120_vs_RI15, **D** RP120_vs_RP15 and (**E**) WI120_vs_WP120. **F** Venn diagram analysis of DECs from 15 and 120 min after insulin/PBS injection in broilers. **G** Venn diagram analysis of DECs detected in RI120_vs_RP120 and WI120_vs_WP120. **H** Expression levels (TPM values) of three common DECs shared by two breeds (as presented in Figure G) after insulin administration. For easy identification, the expression values of the same circRNA across groups are connected by the same color dashed line. "TPM" on y- axis represents "transcript per million". The circINSR is marked out with black arrows in (A) and (C)

Meanwhile, KEGG pathway, such as insulin signaling, MAPK signaling, vascular endothelial growth factor (VEGF) signaling, and the FOXO pathway were enriched in insulin- administrated broilers (Fig. 6A-C, Table S8).

However, there were obvious differences for the enriched GO/KEGG terms between Silky fowls and broilers at 120 min after insulin administration (Figs. 5B and 6C, and 6E, Table S7 and S8). In the WI120_vs_WP120 comparison, the most abundant GO terms were related to the regulation of intracellular signal transduction and erythrocyte differentiation (Fig. 5B, Table S7), and the prominent KEGG signaling pathway was associated with endocytosis regulation, the actin cytoskeleton and MAPK signaling (Fig. 6E, Table S8).

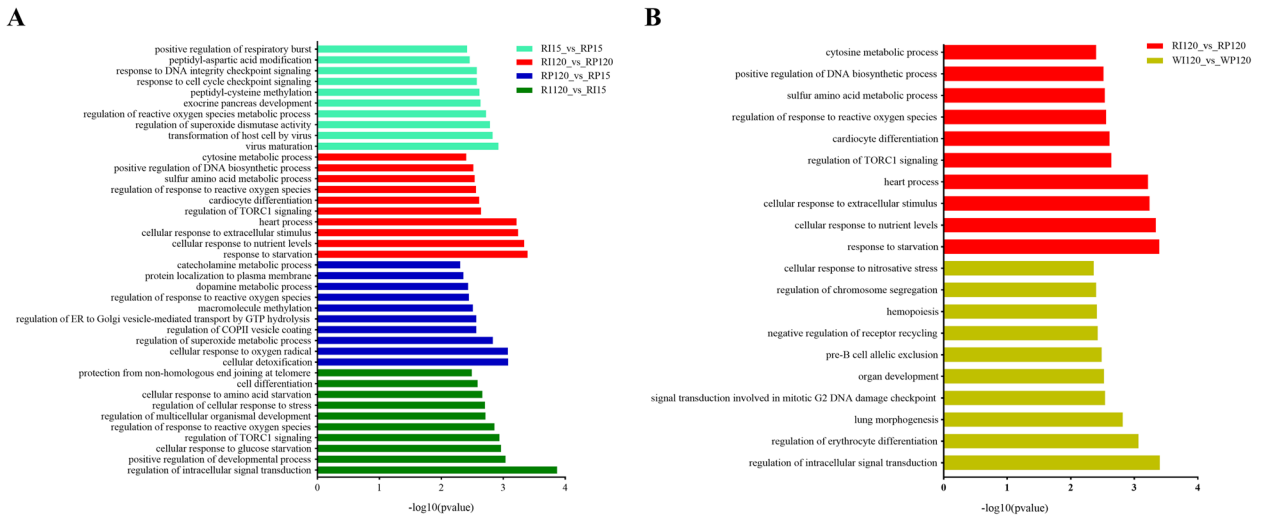

Fig. 5 Gene ontology (GO) enrichment analysis with the source genes of DECs in each comparison. **A** The top 10 GO terms (biological processes) for comparisons from 15 and 120 min after insulin administration in broilers. **B** Comparison of the enriched GO terms between broilers and Silky fowls at 120 min after insulin administration

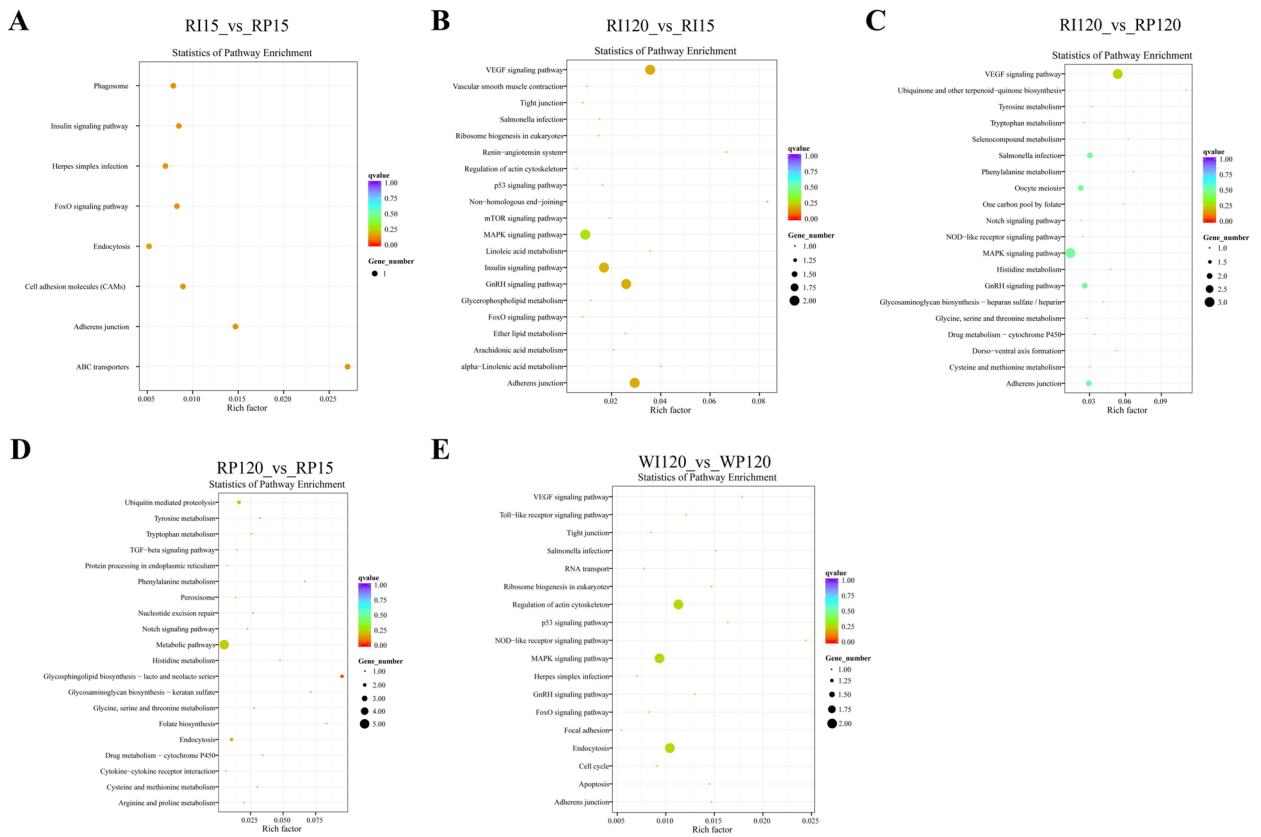

Fig. 6 The Kyoto Encyclopedia of Genes and Genomes (KEGG) classification for the source gene of circRNAs in each comparison. **A** RI15_vs._RP15. **B** RI120_vs._RI15. **C** RI120_vs._RP120. **D** RP120_vs._RP15. **E** WI120_vs._WP120. The top 20 enriched pathway are displayed. If the enrichment terms are less than 20, all of them are displayed

Function prediction on translation and miRNA binding potential of circRNAs

It has been reported that some circRNAs may contain internal ribosome entry sites (IRES) and rely on them for translation [51]. Therefore, we predicted the potential IRES elements based on the identified circRNA sequences. The results showed that 71.73% of circRNAs had translation potential (score > 0.5), among which 8.04% of circRNAs had scores between 0.9 and 1.0 (Fig. 7A). Furthermore, 71 circRNAs with translation potential were identified to be insulin sensitive (Table S6).

CircRNAs can regulate gene expression by acting as a miRNA sponge [48]. It was predicted that most circRNAs contain multiple miRNA binding sites and can interact with numerous miRNAs, primarily ranging from 21 to 40 (Fig. 7B). Notably, one circRNA could bind to as many as 120 miRNAs (Fig. 7B). A complex circRNA-miRNA interaction network was constructed (Fig. 7C). It indicating these circRNAs may function through intricate circRNA-miRNA interaction.

Spatio-temporal expression characteristics of circINSR and *INSR* in two breeds

The insulin receptor binds to insulin and initiates a cascade of events in insulin- target tissues. The activated insulin receptor serves as the gateway for regulating various cellular processes, including glycogen storage, glucose transport, apoptosis, and autophagy [52]. A circRNA (circ_0004546, circINSR, 552 bp) derived from exon 2 of *INSR* (ENSGALT00010066079.1) was identified from the ssRNA-Seq data (Fig. S1E and S3). The circINSR is located within the constructed circRNA-miRNA regulatory network and contains abundant miRNA binding sites (Fig. 7C). It was predicted to have weak translation potential by the IRES finder (score < 0.34).

The spatiotemporal expressions of circINSR and its parental gene *INSR* were investigated in broilers and Silky fowls. It was observed that circINSR widely expressed in the detected tissues (Fig. 8). In broilers, circINSR was predominantly expressed in the pectoralis and leg muscles, with relatively low expression in other detected tissues (Fig. 8A). In contrast, Silky fowls exhibited a broader expression profile for circINSR, with high levels in the pectoral and leg muscles, as well as the pancreas, and relatively low levels in the muscular stomach, glandular stomach, and brain (Fig. 8E). In both broilers and Silky fowls, the levels of circINSR and *INSR* in pectoralis muscle were found to be the lowest at E10 ($P < 0.05$). However, they displayed a dramatic elevation in pectoralis muscle during the later stage of embryonic development and after birth, coinciding with the rapid growth phase of skeletal muscle (Fig. 8B and F). This suggests a conserved role for both circINSR and *INSR* in muscle development and growth across breeds. The expression pattern of the parental gene *INSR* was generally similar to that of circINSR (Fig. 8C, D, G and H). In addition, compared to Silky fowls, broilers exhibited relatively lower levels of circINSR in the pancreas ($P < 0.01$) and higher levels of both circINSR ($P < 0.05$) and *INSR* ($P < 0.01$) in the leg muscle (Fig. 8I-J).

Response of circINSR and *INSR* on exogenous stimuli

We further investigated the response of circINSR and *INSR* to several exogenous stimuli in broilers. First, we evaluated the effect of exogenous insulin on the dynamic change of circINSR and *INSR* in pectoralis of broilers. Along with the dramatical drop of blood glucose following insulin administration (Fig. 9A), the expression of circINSR was deeply inhibited by exogenous insulin at the early stage (15 min) in the pectoralis of broilers (approximately 1/7 of the control birds, $P < 0.01$, Fig. 9D). However, the level of circINSR recovered to the baseline level (0 min) or its PBS control level at 120 min/240 min after insulin stimulation. There was no significant difference in the circINSR level between insulin-treated and PBS control broilers at 120 and 240 min (Fig. 9D). The *INSR* level was also down-regulated by insulin administration at 15 min (1/2 of control birds, $P < 0.05$). However, unlike circINSR, *INSR* level fluctuated over time in PBS control birds ($P < 0.05$) and insulin administration completely reversed the expression pattern of *INSR* at the monitored time points ($P < 0.05$). Compared with the corresponding PBS control, the expression of *INSR* was significantly up-regulated at 120 min ($P < 0.01$) and down-regulated at 240 min by insulin ($P < 0.05$, Fig. 9G).

In pyruvate tolerance tests, the concentration of blood glucose gradually increased over time (0–60 min) following pyruvate administration ($P < 0.05$, Fig. 9B). Nevertheless, the expressions of both circINSR and *INSR* were not significantly changed in the bird's pectoralis after injection of sodium pyruvate (Fig. 9E and 9H). In glucose tolerance tests, a peak in blood glucose level of birds was observed 10 min after glucose injection (Fig. 9C). Meanwhile, the expression of *INSR* was significantly downregulated at 10 min after glucose injection in the pectoralis of birds (Fig. 9I). However, the expression of the circINSR remained relatively stable in bird's pectoralis under glucose administration (Fig. 9F).

Nutritional status can regulate the expression level of target genes. We investigated the impact of feed restriction on the expression of circINSR and *INSR*. It was observed that 15% energy restriction significantly upregulated the expression of circINSR in the pectoralis of broilers ($P < 0.01$, Fig. 10A). However, the relative expression of circINSR was not affected by 15% protein restriction. In addition, unlike circINSR, neither energy nor

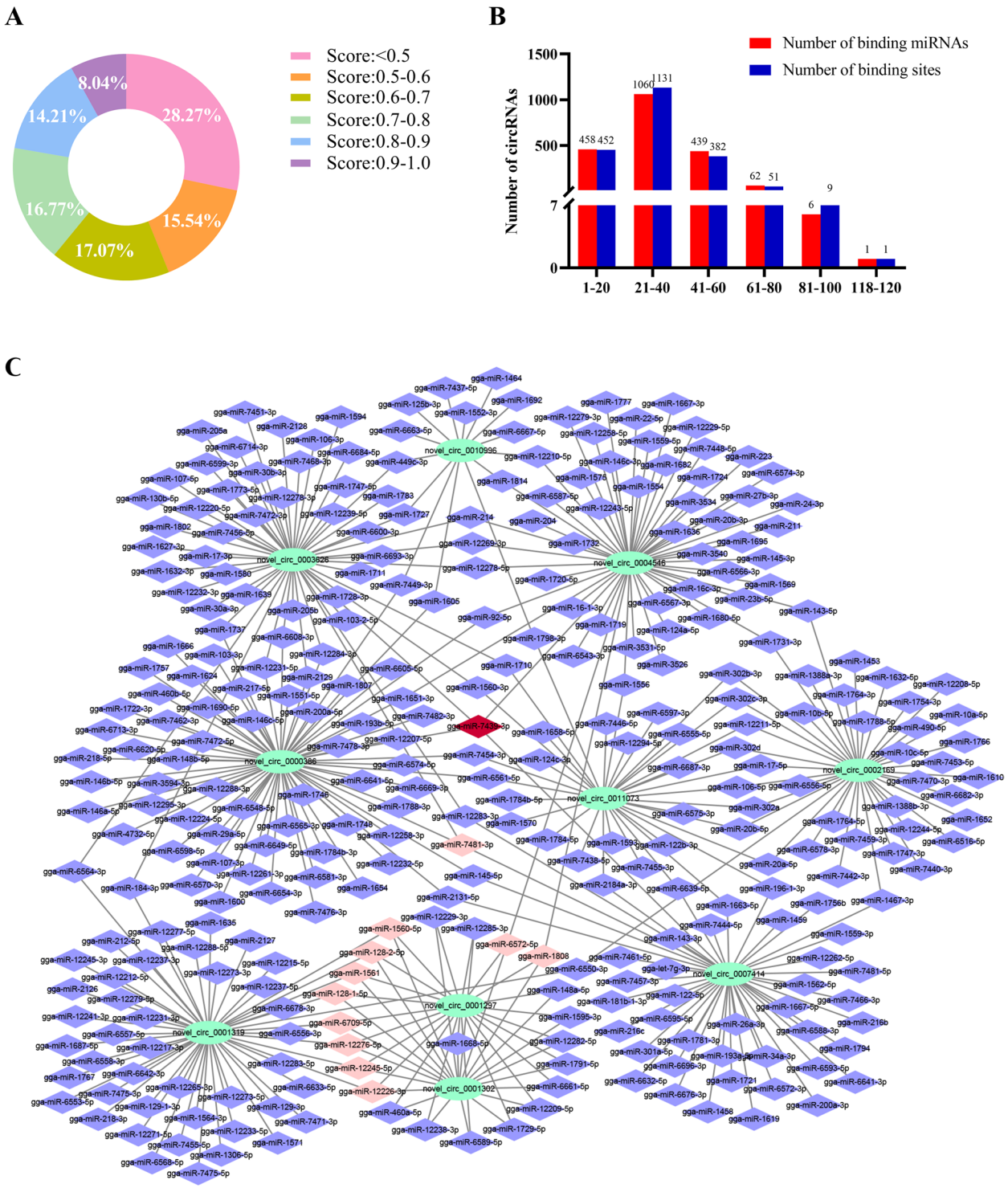

Fig. 7 Function prediction of circRNAs. **A** Prediction of the potential of circRNAs to encode proteins. **B** Statistics on the predicted number of miRNAs binding to circRNAs. The X-axis represents the number of miRNAs, and the Y-axis represents the number of circRNAs that can bind to a certain number of miRNAs. **C** Constructed circRNA-miRNA regulatory network based on the top 10 DECs in the comparisons. The miRNAs that can bind to four circRNAs are shown in red, and those can bind to three circRNAs are shown in pink respectively

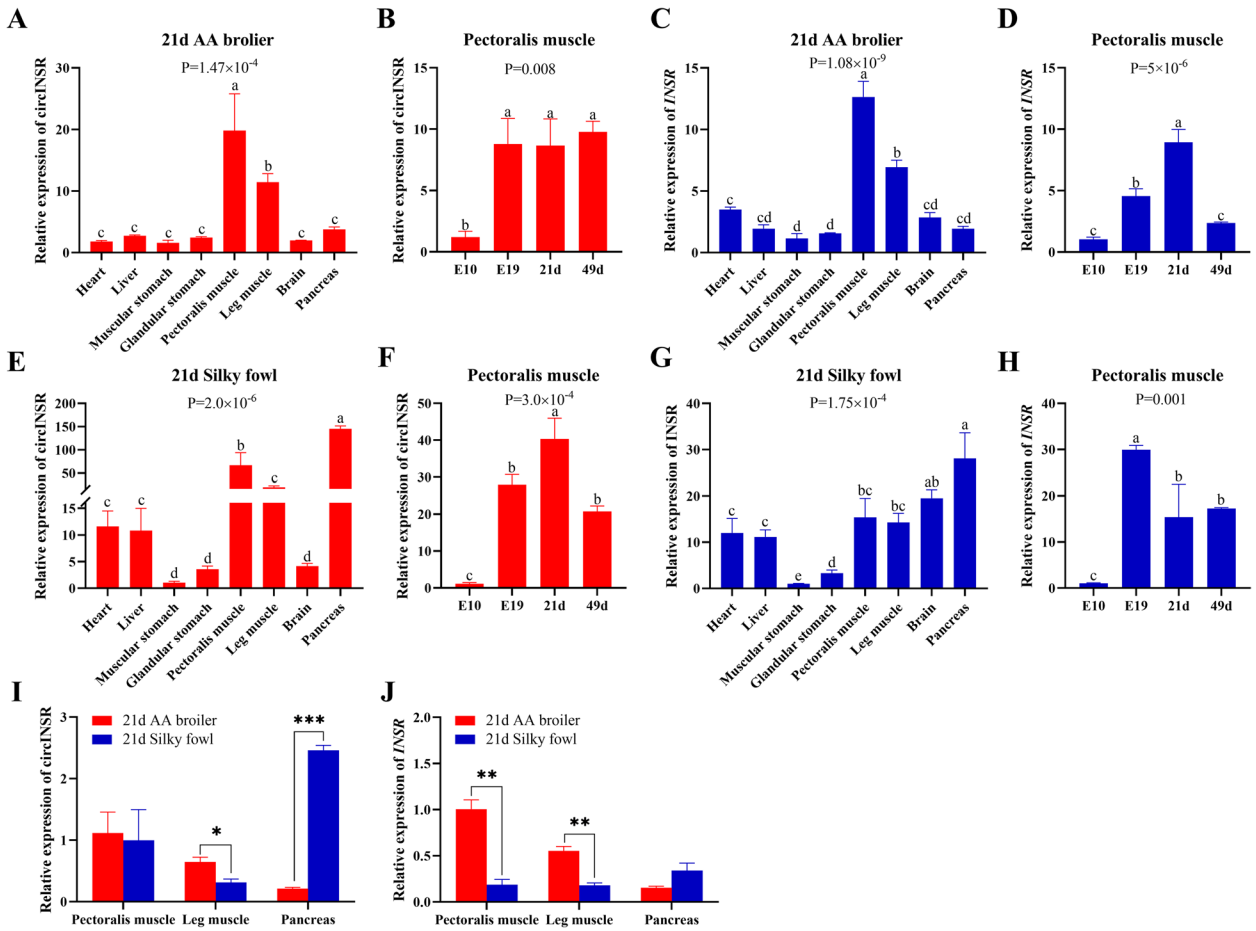

Fig. 8 The expression characteristics of circINSR and its source gene *INSR* in basal state. The tissue expression profiling of circINSR in broilers (**A**) and Silky fowls (**E**), and of *INSR* in broilers (**C**) and Silky fowls (**G**). The temporal expression of circINSR in pectoralis of broilers (**B**) and Silky fowls (**F**), and of *INSR* in pectoralis of broilers (**D**) and Silky fowls (**H**). The expression of circINSR (**I**) and *INSR* (**J**) in pectoralis, leg muscle and pancreas of broilers and Silky fowls. [a,b] Different lowercase letters indicate $P < 0.05$, while the same letter indicates $P > 0.05$. *, $P < 0.05$; **, $P < 0.01$, ***, $P < 0.01$

protein restriction altered the relative expression level of muscle *INSR* (Fig. 10B).

Discussion

In this study, we identified a substantial number of novel circRNAs from bird's pectoralis using ssRNA-Seq. Notably, our samples were not pre-treated with RNase R, which could potentially introduce some bias. RNase R treatment degrades linear transcripts from total RNA, potentially enhancing the detection rate of circRNAs. However, this treatment might also reduce the detection rate of low-abundance circRNAs and lead to an overestimation of intron-derived circRNAs, as lariats are resistant to RNase R treatment [16, 45]. Therefore, to capture all potential circRNAs expressed in bird's pectoralis, we opted to use RNase R- untreated samples. To further validate the circularity and relative abundance of seven circRNAs, we employed RNase R treatment followed by qRT-PCR.

Chromosome 7 is a Hotspot for RNA Cyclizing Events

Interestingly, chromosome 7 in birds appeared to be a hotspot for RNA cyclizing events. Three circRNAs with the highest TPM values were located on chromosome 7. Additionally, the average detection rate of circRNAs on chromosome 7 was relatively higher (3.54/Mb) compared to the genomic level in the bird's pectoralis, which was 1.93/Mb ($P < 0.001$, Chi square test, Fig. S1). Our findings are consistent with the ssRNA-Seq data presented by Shen et al. [22], where the number of circRNAs on chromosome 7 (NC_006127.4, 5.17/Mb) was also more abundant than at the genomic level (3.90/Mb) in the pectoralis muscle of embryonic stage birds. This suggests a potential regional preference for circRNA formation on chromosome 7, which warrants further investigation to understand the underlying mechanisms and functional implications.

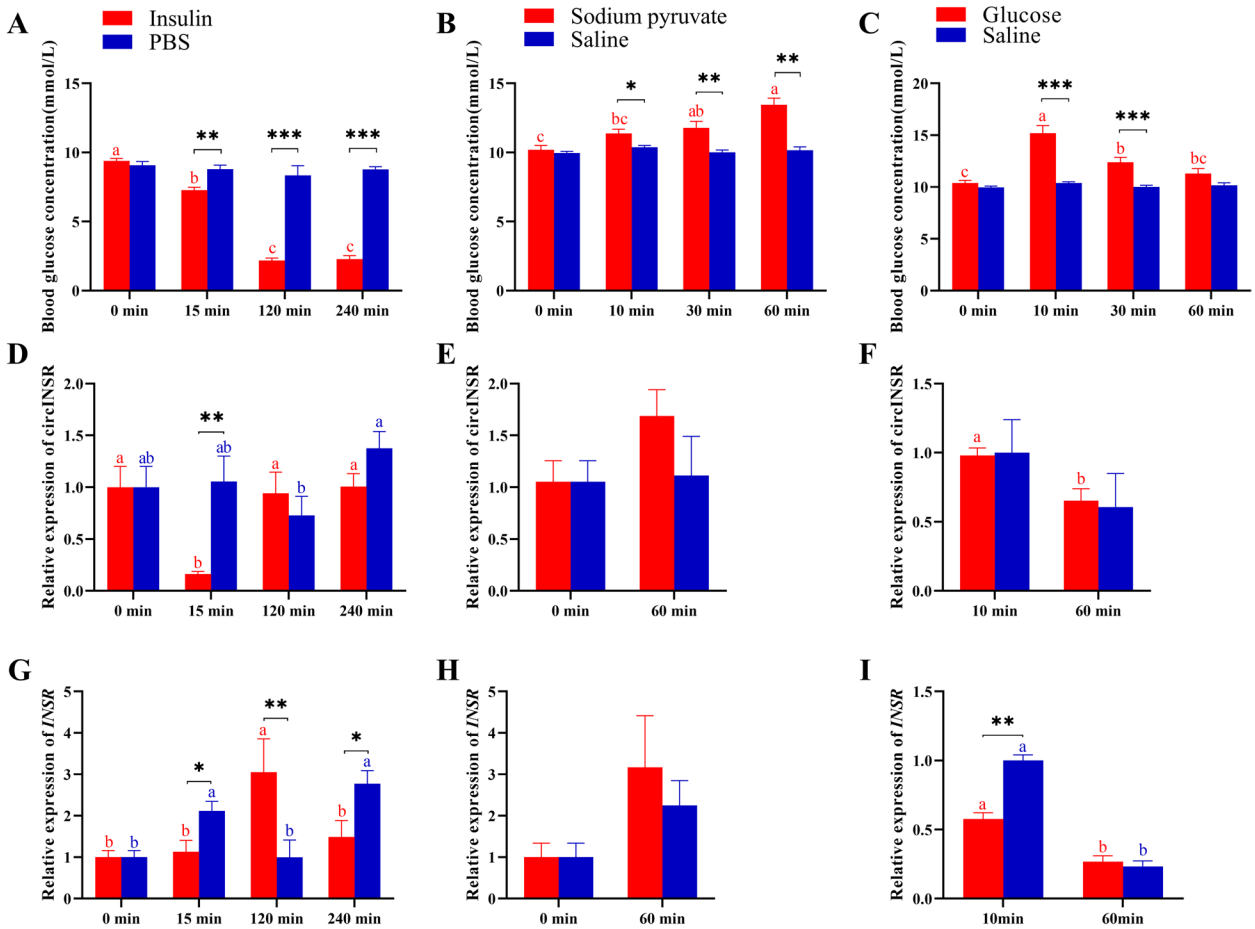

Fig. 9 Effect of exogenous stimuli on the blood glucose and expression of circINSR/INSR in pectoralis of broilers. Effect of insulin (**A**), sodium pyruvate (**B**) and glucose (**C**) treatment on blood glucose concentration in broilers. Effect of insulin on the expression of circINSR (**D**) and *INSR* (**G**). Effect of sodium pyruvate on the expression of circINSR (**E**) and *INSR* (**H**). Effect of glucose on the expression of circINSR (**F**) and *INSR* (**I**). Different red letters indicate $P < 0.05$ among time points after insulin/sodium pyruvate/glucose treatment. Different blue letters indicate $P < 0.05$ among time points after PBS/saline injection (as control). Between treatment and control groups at a specific time point, * indicates $P < 0.05$; ** indicates $P < 0.01$. The same letters or no labels indicate $P > 0.05$. The broilers were intraperitoneally injected with insulin at a dose of 5 IU/kg body weight at 24 d, and PBS- injected broilers served as control. Broilers were intraperitoneally injected with a 10% glucose solution at a dose of 2 g/kg body weight at 18 d, and with a sodium pyruvate solution at a dose of 2 g/kg body weight at 21 d, and the control broilers were injected with the same dose of normal saline

Insulin-responsive circRNAs: key regulators of glucose homeostasis in birds through miRNA-mediated pathways

Insulin is a key player in animal physiology, acting not only as a regulator of glucose homeostasis in animals [11], but also as a potent anabolic factor that sustains muscle growth in organisms. By binding to specific receptors (*INSR*), insulin activates a cascade of phosphorylation events, leading to the enhancement of protein synthesis and inhibition of protein breakdown [12]. The identified insulin-responsive circRNAs are the potential regulators of glucose homeostasis and muscle development in animals.

Previous studies have reported a linear decrease in blood glucose levels in chickens over time (0–120 min) following exogenous insulin stimulation [34, 35]. Our research, using ssRNA-Seq, further revealed the involvement of abundant circRNAs in insulin-mediated regulation within the pectoral muscles of birds. These insulin-sensitive circRNAs function in a time-specific and breed-specific manner under insulin administration. Notably, fewer DECs are shared between the early stage (15 min) and later stage (120 min) in broilers, as well as between broilers and Silky fowls at 120 min. This may contribute to the differential glucose homeostatic regulation [34] Specifically, three commonly down-regulated circRNAs by insulin at 120 min (novel_circ_0004076, novel_circ_0010996 and novel_circ_0001431) in two breeds, may play a positive role in blood glucose regulation in a breed-independent manner. Therefore, further research is needed to explore their function on insulin-mediated glucose homeostasis.

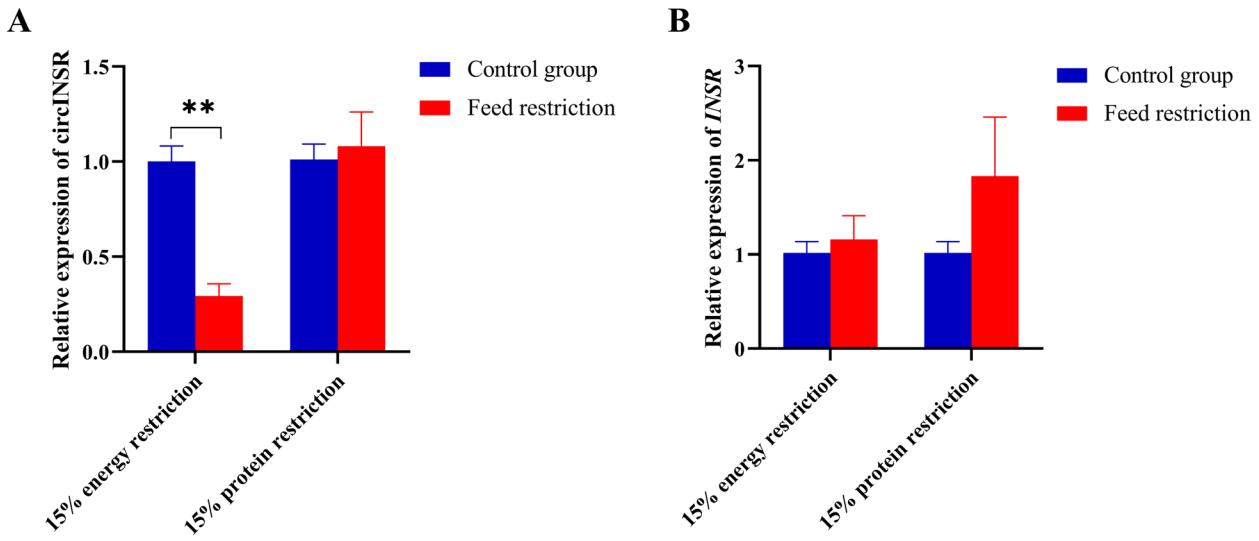

Fig. 10 Feed restriction on the expression of circINSR and its original gene *INSR*. **A** circINSR. **B** *INSR*

CircRNAs can serve as miRNA sponges and interacting with miRNAs to regulate gene expression. In the constructed miRNA-circRNA regulatory network (Fig. 7), some miRNAs have been reported to be involved in insulin-related metabolism. For example, miR-103 and miR-107 directly regulate insulin sensitivity in adipocytes [35, 53]. Knockdown of miR-143 or miR-145 in vascular smooth muscle cells induces the expression of insulin receptor substrate 1 and increases glucose uptake [54]. Additionally, miR-26a enhances insulin sensitivity, decreases glucose production, and reduces fatty acid synthesis in mice [55]. These findings suggested that circRNAs identified in our study may be involved in insulin pathway by binding to these miRNAs. Further research is needed to identify the functions of these insulin-sensitive circRNAs and their interaction with corresponding miRNAs.

CircINSR: a conserved and insulin-responsive circRNA with dual roles in glucose homeostasis and muscle development across species

A circRNA (circINSR) formed by the exon 2 of linear *INSR* (552 bp) was identified from chicken pectoralis through ssRNA-Seq. This circRNA is highly conservative across species, including humans (has_circ_0048966 in circBase, http://www.circbase.Org), mice, and bovines [56]. It shares about 77% similarity between chicken and mammals, and even 89% similarity among mammals (Fig. S3), suggesting circINSR likely has important and conservative functions across species.

INSR is a transmembrane receptor that can be activated by insulin, playing a key role in the regulation of glucose homeostasis metabolically and muscle development [57–59]. The β-cell-specific *INSR* deletion can lead to insulin hypersecretion and improve glucose tolerance before the onset of global insulin resistance [60]. In chicken, circINSR exhibits high expression levels in skeletal muscles and dynamic expression during development, indicating its potentially significant role in muscle development as *INSR*. It has been reported that bovine circINSR can promote the proliferation and reduce the apoptosis of embryonic myoblasts by sponging miR-34a, serving as a regulator of embryonic muscle and intramuscular fat development [56, 61].

Although circINSR and *INSR* exhibit similar spatiotemporal expression pattern in the basal state, circINSR shows a distinct modulation from *INSR* under exogenous stimulations in bird's pectoralis. CircINSR, like its parental gene *INSR*, is an insulin-responsive gene. However, circINSR appears to function primarily as an early insulin-responder, playing a positive role in the early phase of blood glucose reduces mediated by insulin. In contrast, *INSR* has distinct roles in the early and later phases of blood glucose modulation induced by exogenous insulin. The dynamic change in *INSR* further demonstrated its crucial function in maintaining glucose homeostasis in birds. Additionally, circINSR in birds seems to be more sensitive to energy reduction than that of *INSR*, suggesting that circINSR and *INSR* may play independent and overlapping roles in insulin signaling cascade.

After insulin and glucose administration, Silky fowls show a more rapid return to normal blood sugar levels compared to broilers [33, 34]. This glucose homeostasis is largely maintained by pancreatic β-cells, which secrete insulin, as a crucial player in this process [62]. Notably, in Silky fowls, there is a high expression of both circINSR and *INSR* in the pancreas, which may enhance the role

of pancreatic β-cells and thereby boosting glucose homeostasis.

Furthermore, circINSR likely have other important functions. It has been reported that the sheep circINSR can inhibit adipogenic differentiation of adipose-derived stromal vascular fractions through the miR-152/MEOX2 axis [63]. Additionally, it can protect against doxorubicin-induced cardiotoxicity [64]. Further research is needed to clarify the function of and its regulation mechanism.

Additionally, circSZT2, the only insulin-sensitive DECs shared by two time- points in the pectoralis tissues of broilers (Fig. 4F), displays a dynamic regulation with the changes in blood glucose under insulin administration (Fig. 3), but in a manner opposite to *INSR* (Fig. 9G). This suggested that circSZT2 may play a key role in glucose homeostasis. The potentially important function of bird's circSZT2 in the insulin-involved signaling cascade warrants further investigation.

It is important to note that, due to resource and logistical constraints, only single-sex birds were used in this study, which may introduce some sex-related bias. However, this approach can effectively minimize potential confounding effects caused by sex-related differences, ensuring greater consistency and reliability in the experimental outcomes. Additionally, this study provides the investigation into the early-phase and dynamic modulation patterns of circRNAs in response to insulin in rapidly growing broilers using ssRNA-Seq, offering valuable insights into the potential roles of circRNAs in insulin-mediated glucose homeostasis. However, breed-specific differences may exist and warrant further exploration. Despite its limitations, our study successfully identified a substantial number of novel insulin-sensitive circRNAs and revealed their potential roles in insulin-mediated glucose homeostasis. These findings lay a foundation for further research into circRNA-mediated regulation of glucose homeostasis.

Conclusion

This study identified abundant insulin-sensitive circRNAs in the pectoralis muscle of birds using ssRNA-Seq, revealing their time-specific and breed-specific regulation by exogenous insulin. These circRNAs, particularly circINSR, play crucial roles in glucose homeostasis and muscle development through the insulin signaling cascade. CircINSR, an early insulin responder, exhibits distinct and overlapping expression patterns compared to its source gene *INSR* and is downregulated by insulin and energy restriction. These findings provide novel insights into the regulatory mechanisms of insulin action from the perspective of circRNAs, highlighting their potential importance in metabolic and developmental processes in birds.

Abbreviations

circRNAs	Circular RNAs
ssRNA-Seq	Strand-specific RNA sequencing
AA broilers	Arbor Acres broilers
INSR	Insulin receptor
DECs	Differentially expressed circRNAs
IRES	Internal ribosome entry site
gDNA	Genomic DNA
GO	Gene ontology
KEGG	The Kyoto Encyclopedia of Genes and Genomes

Supplementary Information

The online version contains supplementary material available at https://doi.org/10.1186/s12864-025-11347-w.

Additional file 1: Fig. S1. Profilings of circRNAs in chicken pectoralis muscles. (A) Classification of identified circRNAs. (B) Distribution of exon-derived circRNAs. (C) The circRNAs distribution in each chromosome. (D) The correlation between chromosome length (Mb) and the number of detected circRNAs. (E) The schematic diagram of circINSR structure. The genomic structure of *INSR* was based on ENSGALT00010066079.1. The arrow indicates the junction site.

Supplementary Material 2: Fig. S2. Expression analysis of circRNAs in each sample. (A) The density of circRNAs expression in each sample. (B) Box plot of circRNAs expression in each sample. (C) Cluster heat-map of differential circRNAs. where "TPM" on y- axis represents "transcript per million".

Supplementary Material 3: Fig. S3. Conservation of circINSR across chicken, human, and mouse. Bases identical to chicken circINSR sequence are indicated in a dash.

Supplementary Material 4: Table S1. Diet formula for restricted population (air-dry basis).

Supplementary Material 5: Table S2. Diet formula for other experimental birds (air-dry basis).

Supplementary Material 6: Table S3. Primer information for amplifying the corresponding genes.

Supplementary Material 7: Table S4. All circRNAs identified from 18 cDNA libraries.

Supplementary Material 8: Table S5. The information of 6 circRNAs formed by MAPK1.

Supplementary Material 9: Table S6. The information about 71 insulin-sensitive circRNAs possessing translational potential.

Supplementary Material 10: Table S7. Enriched GO pathway in each comparison.

Supplementary Material 11: Table S8. Enriched KEGG Terms in each comparison.

Acknowledgements

Not applicable.

Authors' contributions

YQH conceived and designed the research. BHS performed the experiments and wrote the manuscript. ZYW prepared the material and wrote the manuscript. PNL, PFD, XLZ, HYZ, XMS and SM revised the paper; YQH and WC acquired project funding. All the authors have read and approved the final manuscript.

Funding

This study was financially supported by the National Natural Science Foundation of China (32,072,748) and Key project of Natural Science Foundation of Henan Province (232,300,421,109).

Data availability

ssRNA-seq data have been deposited in SRA database under accession number PRJNA1039253, PRJNA1039241 and PRJNA1039316. All additional data produced or examined during this research can be found within the manuscript and its supplementary files.

Declarations

Ethics approval and consent to participate
The animal experiment scheme was approved by the Institutional Animal Care and Use Committee of Henan Agricultural University (HNND-2021–104, Zhengzhou, Henan, China). All animal experiments performed in this study comply fully with animal welfare regulations.

Consent for publication
Not applicable. The authors declare that they have no known competing financial interests or personal relationships that could have appeared to influence the work reported in this paper.

Competing interests
The authors declare no competing interests.

Received: 25 September 2024 Accepted: 10 February 2025
Published online: 15 February 2025

References

1. Chen I, Chen C-Y, Chuang T-J. Biogenesis, identification, and function of exonic circular RNAs. Wiley Interdiscip Rev RNA. 2015;6(5):563–79.
2. Hentze MW, Preiss T. Circular RNAs: splicing's enigma variations. Embo J. 2013;32(7):923–5.
3. Suzuki H, Zuo Y, Wang J, Zhang MQ, Malhotra A, Mayeda A. Characterization of RNase R-digested cellular RNA source that consists of lariat and circular RNAs from pre-mRNA splicing. Nucleic Acids Res. 2006;34(8):e63–e63.
4. Chen R, Lei S, Jiang T, Zeng J, Zhou S, She Y. Roles of lncRNAs and circRNAs in regulating skeletal muscle development. Acta Physiol. 2019;228(2):e13356.
5. Yan J, Yang Y, Fan X, Liang G, Wang Z, Li J, Wang L, Chen Y, Adetula AA, Tang Y, et al. circRNAome profiling reveals circFgfr2 regulates myogenesis and muscle regeneration via a feedback loop. J Cachexia Sarcopenia. 2022;13(1):696–712.
6. Arcinas C, Tan W, Fang W, Desai TP, Teh DCS, Degirmenci U, Xu D, Foo R, Sun L. Adipose circular RNAs exhibit dynamic regulation in obesity and functional role in adipogenesis. Nat Metab. 2019;1(7):688–703.
7. Ashwal-Fluss R, Meyer M, Pamudurti NR, Ivanov A, Bartok O, Hanan M, Evantal N, Memczak S, Rajewsky N, Kadener S. circRNA biogenesis competes with pre-mRNA splicing. Mol Cell. 2014;56(1):55–66.
8. Du WW, Yang W, Liu E, Yang Z, Dhaliwal P, Yang BB. Foxo3 circular RNA retards cell cycle progression via forming ternary complexes with p21 and CDK2. Nucleic Acids Res. 2016;44(6):2846–58.
9. Zhang J, Li Y, Qi J, Yu X, Ren H, Zhao X, et al. Circ-calm4 serves as an miR-337-3p sponge to regulate Myo10 (Myosin 10) and promote pulmonary artery smooth muscle proliferation. Hypertension. 2020;75(3):668–79.
10. Pan Z, Cai J, Lin J, Zhou H, Peng J, Liang J, et al. A novel protein encoded by circFNDC3B inhibits tumor progression and EMT through regulating snail in colon cancer. Mol Cancer. 2020;19(1):71.
11. Haeusler RA, McGraw TE, Accili D. Biochemical and cellular properties of insulin receptor signalling. Nat Rev Mol Cell Bio. 2018;19(1):31–44.
12. Sartori R, Romanello V, Sandri M. Mechanisms of muscle atrophy and hypertrophy: implications in health and disease. Nat Commun. 2021;12(1):330.
13. Meng ZX, Gong J, Chen Z, Sun J, Xiao Y, Wang L, et al. Glucose sensing by skeletal myocytes couples nutrient signaling to systemic homeostasis. Mol Cell. 2017;66(3):332-44.e4.
14. Stoll L, Sobel J, Rodriguez-Trejo A, Guay C, Lee K, Venø MT, et al. Circular RNAs as novel regulators of β-cell functions in normal and disease conditions. Mol Metab. 2018;9:69–83.
15. Sun R, Xue W, Zhao J. Hsa_circ_0054633 mediates apoptosis and insulin secretion in human pancreatic β cells through miR-409-3p/caspase-8 axis. Diabetes Res Clin Pr. 2021;176: 108837.
16. Stoll L, Rodríguez-Trejo A, Guay C, Brozzi F, Bayazit M, Gattesco S, et al. A circular RNA generated from an intron of the insulin gene controls insulin secretion. Nat Commun. 2020;11(1):5611.
17. Liu Y, Yang Y, Xu C, Liu J, Chen J, Li G, et al. Circular RNA circGlis3 protects against islet β-cell dysfunction and apoptosis in obesity. Nat Commun. 2023;14(1):351.
18. Yan YX, Dong J, Li YL, Lu YK, Yang K, Wang T, et al. CircRNA hsa_circ_0071336 is associated with type 2 diabetes through targeting the miR-93-5p/GLUT4 axis. Faseb J. 2022;36(5): e22324.
19. Lu YK, Chu X, Wang S, Sun Y, Zhang J, Dong J, et al. Identification of circulating hsa_circ_0063425 and hsa_circ_0056891 as novel biomarkers for detection of type 2 diabetes. J Clin Endocrinol Metab. 2021;106(7):e2688–99.
20. Weigelt CM, Sehgal R, Tain LS, Cheng J, Eßer J, Pahl A, et al. An insulin-sensitive circular RNA that regulates lifespan in drosophila. Mol Cell. 2020;79(2):268-79.e5.
21. Shen M, Li T, Zhang G, Wu P, Chen F, Lou Q, et al. Dynamic expression and functional analysis of circRNA in granulosa cells during follicular development in chicken. BMC Genomics. 2019;20(1):96.
22. Shen X, Liu Z, Cao X, He H, Han S, Chen Y, et al. Circular RNA profiling identified an abundant circular RNA circTMTC1 that inhibits chicken skeletal muscle satellite cell differentiation by sponging miR-128-3p. Int J Biol Sci. 2019;15(10):2265–81.
23. Lei Q, Hu X, Han H, Wang J, Liu W, Zhou Y, et al. Integrative analysis of circRNA, miRNA, and mRNA profiles to reveal ceRNA regulation in chicken muscle development from the embryonic to post-hatching periods. BMC Genomics. 2022;23(1):342.
24. Tian W, Zhang B, Zhong H, Nie R, Ling Y, Zhang H, et al. Dynamic expression and regulatory network of circular RNA for abdominal preadipocytes differentiation in chicken (Gallus gallus). Front Cell Dev Biol. 2021;9: 761638.
25. Liu XD, Song J, Liu X, Shan H. Research note: circular RNA expressing in different developmental stages of the chicken bursa of Fabricius. Poult Sci. 2020;99(8):3846–52.
26. Chen D, Miao Z, Peng M, Xing H, Zhang H, Teng X. The co-expression of circRNA and mRNA in the thymuses of chickens exposed to ammonia. Ecotoxicol Environ Safe. 2019;176:146–52.
27. Zhang Y, Wang L, Qiu L, Pan R, Bai H, Jiang Y, et al. Expression patterns of novel circular RNAs in chicken cells after avian leukosis virus subgroup J infection. Gene. 2019;701:72–81.
28. Zheng L, Liu L, Lin L, Tang H, Fan X, Lin H, et al. Cecal circRNAs are associated with the response to salmonella enterica serovar enteritidis inoculation in the chicken. Front Immunol. 2019;10:1186.
29. Wang L, You Z, Wang M, Yuan Y, Liu C, Yang N, et al. Genome-wide analysis of circular RNAs involved in Marek's disease tumourigenesis in chickens. RNA Biol. 2020;17(4):517–27.
30. Chen L, Li G, Tian Y, Zeng T, Xu W, Gu T, et al. RNA sequencing reveals circRNA expression profiles in chicken DF1 cells infected with H5N1 influenza virus. Animals. 2022;12(2):158.
31. Braun EJ, Sweazea KL. Glucose regulation in birds. Comp Biochem Physiol B Biochem Mol Biol. 2008;151(1):1–9.
32. Sumners LH, Zhang W, Zhao X, Honaker CF, Zhang S, Cline MA. Animals chickens from lines artificially selected for juvenile low and high body weight differ in glucose homeostasis and pancreas physiology. Comp Biochem Physiol A Mol Integr Physiol. 2014;172:57–65.
33. Du P, Wang H, Shi X, Zhang X, Zhu Y, Chen W, et al. A comparative study to determine the effects of breed and feed restriction on glucose metabolism of chickens. Anim Nutr. 2023;13:261–9.
34. Ji J, Tao Y, Zhang X, Pan J, Zhu X, Wang H, et al. Dynamic changes of blood glucose, serum biochemical parameters and gene expression in response to exogenous insulin in Arbor Acres broilers and Silky fowls. Sci Rep Uk. 2020;10(1):6697.
35. Wang H, Du P, Zhang J, Zhu Y, Ji J, Chen W, et al. Effect of insulin injection on blood glucose concentration and feeding status of different breed chickens. Chin J Anim Nutr. 2020;32:2164–75.
36. Gilbert ER, Fu Z, Liu D. Development of a nongenetic mouse model of type 2 diabetes. Exp Diabetes Res. 2011;2011: 416254.
37. Ferreira DS, Amaral FG, Mesquita CC, Barbosa AP, Lellis-Santos C, Turati AO, et al. Maternal melatonin programs the daily pattern of energy metabolism in adult offspring. PLoS One. 2012;7(6): e38795.
38. Yang S, Li M, Xia M, Shang Y, Chen Y, Lu B, et al. Effects of different feed restriction methods on growth performance, slaughter performance and skeletal traits of Arbor Acres chicken. Chin J Anim Nutr. 2017;29(09):3341–51.

39. Langmead B, Trapnell C, Pop M, Salzberg SL. Ultrafast and memory-efficient alignment of short DNA sequences to the human genome. Genome Biol. 2009;10(3): R25.
40. Memczak S, Jens M, Elefsinioti A, Torti F, Krueger J, Rybak A, et al. Circular RNAs are a large class of animal RNAs with regulatory potency. Nature. 2013;495(7441):333–8.
41. Gao Y, Zhang J, Zhao F. Circular RNA identification based on multiple seed matching. Brief Bioinform. 2018;19(5):803–10.
42. Hansen TB, Venø MT, Damgaard CK, Kjems J. Comparison of circular RNA prediction tools. Nucleic Acids Res. 2016;44(6): e58.
43. Zhou L, Chen J, Li Z, Li X, Hu X, Huang Y, et al. Integrated profiling of microRNAs and mRNAs: microRNAs located on Xq27.3 associate with clear cell renal cell carcinoma. PloS One. 2010;5(12): e15224.
44. Wang L, Feng Z, Wang X, Wang X, Zhang X. DEGseq: an R package for identifying differentially expressed genes from RNA-seq data. Bioinformatics. 2010;26(1):136–8.
45. Ma N, Tie C, Yu B, Zhang W, Wan J. Circular RNAs regulate its parental genes transcription in the AD mouse model using two methods of library construction. FASEB J. 2020;34(8):10342–56.
46. Young MD, Wakefield MJ, Smyth GK, Oshlack A. Gene ontology analysis for RNA-seq: accounting for selection bias. Genome Biol. 2010;11(2): R14.
47. Mao X, Cai T, Olyarchuk JG, Wei L. Automated genome annotation and pathway identification using the KEGG Orthology (KO) as a controlled vocabulary. Bioinformatics. 2005;21(19):3787–93.
48. Hansen TB, Jensen TI, Clausen BH, Bramsen JB, Finsen B, Damgaard CK, et al. Natural RNA circles function as efficient microRNA sponges. Nature. 2013;495(7441):384–8.
49. Baird SD, Lewis SM, Turcotte M, Holcik M. A search for structurally similar cellular internal ribosome entry sites. Nucleic Acids Res. 2007;35:4664–77.
50. Livak KJ, Schmittgen TD. Analysis of relative gene expression data using real-time quantitative PCR and the 2(-delta delta C(T)) Method. Methods. 2001;25(4):402–8.
51. Legnini I, Di Timoteo G, Rossi F, Morlando M, Briganti F, Sthandier O, et al. Circ-ZNF609 is a circular RNA that can be translated and functions in myogenesis. Mol Cell. 2017;66(1):22–37.
52. Scapin G, Dandey VP, Zhang Z, Prosise W, Hruza A, Kelly T, et al. Structure of the insulin receptor-insulin complex by single-particle cryo-EM analysis. Nature. 2018;556(7699):122–5.
53. Trajkovski M, Hausser J, Soutschek J, Bhat B, Akin A, Zavolan M, et al. MicroRNAs 103 and 107 regulate insulin sensitivity. Nature. 2011;474(7353):649–53.
54. Lan S, Albinsson S. Regulation of IRS-1, insulin signaling and glucose uptake by miR-143/145 in vascular smooth muscle cells. Biochem Bioph Res Co. 2020;529(1):119–25.
55. Fu X, Dong B, Tian Y, Lefebvre P, Meng Z, Wang X, et al. MicroRNA-26a regulates insulin sensitivity and metabolism of glucose and lipids. J Clin Invest. 2015;125(6):2497–509.
56. Shen X, Zhang X, Ru W, Huang Y, Lan X, Lei C, et al. circINSR promotes proliferation and reduces apoptosis of embryonic myoblasts by sponging miR-34a. Mol Ther Nucl Acids. 2020;19:986–99.
57. Lee J, Pilch PF. The insulin receptor: structure, function, and signaling. Am J Physiol. 1994;266(2):C319–34.
58. O'Neill BT, Lauritzen HP, Hirshman MF, Smyth G, Goodyear LJ, Kahn CR. Differential role of insulin/IGF-1 receptor signaling in muscle growth and glucose homeostasis. Cell Rep. 2015;11(8):1220–35.
59. O'Neill BT, Lee KY, Klaus K, Softic S, Krumpoch MT, Fentz J, et al. Insulin and IGF-1 receptors regulate FoxO-mediated signaling in muscle proteostasis. J Clin Invest. 2016;126(9):3433–46.
60. Skovsø S, Panzhinskiy E, Kolic J, Cen HH, Dionne DA, Dai X-Q, et al. Beta-cell specific Insr deletion promotes insulin hypersecretion and improves glucose tolerance prior to global insulin resistance. Nat Commun. 2022;13(1):735.
61. Shen X, Tang J, Ru W, Zhang X, Huang Y, Lei C, et al. CircINSR regulates fetal bovine muscle and fat development. Front Cell Dev Biol. 2020;8: 615638.
62. Rorsman P, Ashcroft FM. Pancreatic β-cell electrical activity and insulin secretion: of mice and men. Physiol Rev. 2018;98(1):117–214.
63. Zhao B, Zhang H, Zhao D, Liang Y, Qiao L, Liu J, et al. CircINSR inhibits adipogenic differentiation of adipose-derived stromal vascular fractions through the miR-152/MEOX2 axis in sheep. Int J Mol Sci. 2023;24(4): 3501.
64. Lu D, Chatterjee S, Xiao K, Riedel I, Huang CK, Costa A, et al. A circular RNA derived from the insulin receptor locus protects against doxorubicin-induced cardiotoxicity. Eur Heart J. 2022;43(42):4496–511.

Publisher's Note